J.M. Desse, R. Deron
(Onera)

E-mail: Jean-Michel.Desse@onera.fr

Shadow, Schlieren and Color Interferometry

This article describes the three main methods for visualization of a gas in motion based on local refractive index variations: shadowgraph, schlieren and interferometric techniques. These non-invasive methods have been used by Onera for visualizing and measuring the gas density fields of two-dimensional and axisymmetric flows, varied examples of which are presented here. The originality of this paper lies, on the one hand, in recent developments in polychromatic holographic interferometry using transmission and reflection panchromatic plates and, on the other hand, the results obtained in digital color holographic interferometry. Although the CCD resolution and size are not as good as that of holographic plates, digital three-wavelength holographic interferometry appears, for the near future, to be the best candidate to characterize future complex flows.

Introduction

Fine characterization of complex flows has become an recognized, specific approach since the 1950's. The need to develop measurement tools adapted to the study of aerodynamic flows was already a major concern at the time and, for this reason, specific shadow, schlieren and interferometric optical benches were built in various Onera wind tunnels. Among the optical methods used in fluid mechanics, those based on variations of the refractive index of media have the advantage of being non-invasive, as only luminous phenomena occur. Some of these processes, such as shadow or schlieren techniques, provide information that is most often qualitative, while others, such as interferometry, give access to a property of the fluid, the gas density, if the flow is two-dimensional or axisymmetric.

Shadow technique

Changes in the refractive index of a gas can be made sensitive by using the deviation produced by the light rays through this gas [1]. It is assumed that the refractive index n is independent of z, the z axis being perpendicular to the flow axis. The gas thickness e, the refractive index n and the optical thickness E are functions of x and y. The Malus theorem determines that the deviations θ_x or θ_y produced by the gas are respectively equal to $\delta E / \delta x$ or $\delta E / \delta y$. Light deviations are caused by variations in the refractive index which are directly related to variations in gas density. The visualization methods based on this principle are shadow or schlieren techniques: they are called «methods of deviation.»

In the shadow technique, the test section is crossed mostly by a beam of parallel light. It uses a small source located at the focal length of a converging lens or a spherical concave mirror. After crossing the test section, the beam illuminates a screen placed beyond the test section at a distance b. A beam undergoing a deviation θ will be visualized on the screen at a nearby point where it would be visualized without flow. This deviation depends on the gradient of the gas density. For a uniform gas density gradient, this shift is constant and the screen is evenly lit. However, if the gas density gradient is variable, displacements vary from one point to another and light and dark areas can be observed on the screen. The contrast on the screen is measured by the relative variation of the illumination I and we have:

$$\frac{dI}{I} = -b\frac{dE^2}{dx^2} \quad (1)$$

The shadow technique indicates the second derivative of the optical thickness of the test section, and thus the gas density if the thickness e is constant. The visualization of shock waves gives particularly good results, because the second derivative of the density changes sign. The situation is illustrated in Figure 1 where one can see the flow around a circular cylinder at Mach 0.75 [2] and the phenomenon of the incoming blast wave of a small rifle [3]. In the first case, high speed visualizations synchronized with unsteady pressure measurements show a strong coupling between the flow over the cylinder and the vortex street formed in the near wake. In the second case, the effects produced by the firing of guns are visualized by high-speed shadow technique and a certain number of parameters have been identified to establish the rules of similarity for this phenomenon. Here, the exposure time of each frame is 300 nanoseconds.

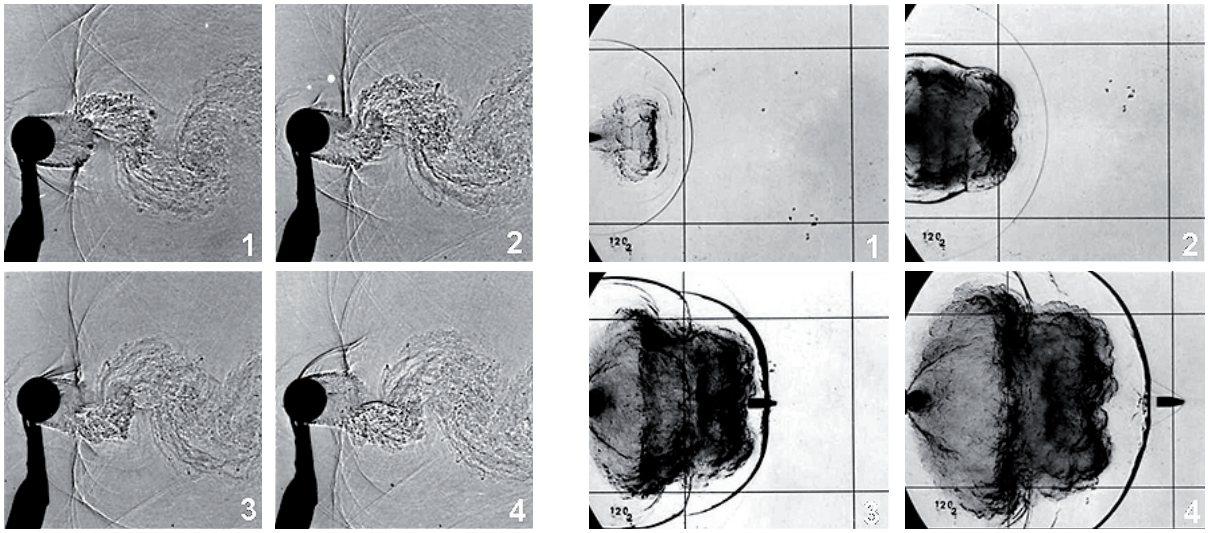

Figure 1 - Visualizations recorded with high-speed shadow technique
Video - http://aerospacelab.onera.org
http://aerospacelab.onera.fr/al1/Shadow-Schlieren-and-Color-Interferometry

Schlieren technique

The schlieren method devised by Foucault and developed by Töpler involves intercepting, with a knife, some of the light rays which are deflected in the test section [4]. In practice, a condenser forms from a source S an image S' which is cut with a knife. A lens located between the screen and S' gives an image of the test section. A part of the light rays passing through S at one point in the test section is intercepted by the knife while the other part A converges on the screen (see Box 1). If the brightness of the source is constant, the irradiance I is proportional to the beam of light that is stopped by the knife. When the rays are not deflected, section A does not change regardless of the point of the screen. The illumination is uniform and I proportional to S' which emerges from the knife. When the optical thickness of the test section varies, section A varies as a result of deviations of the light beams. The variation dI depends on θ_x, because the illumination I is proportional to part A. If b is the distance from the knife to the section and h the height of section A in the absence of variation, it is shown that:

$$\frac{dI}{I} = \frac{dA}{A} = \frac{b}{h}\theta_x = \frac{b}{h}\frac{dE}{dx} \qquad (2)$$

We see that the schlieren method shows the first derivative of the gas density if the flow is two-dimensional and if the test section walls are parallel. Two examples are given in Figure 2. First, a comparison of the shadow and schlieren techniques shows the flow instabilities on the upper side of an airfoil at Mach 0.76 (8° attack angle). Schlieren pictures reveal fine structures, especially downstream from the shock wave and in the separated flow. The schlieren technique can be also applied in a water tunnel. The picture in Figure 2 shows the wake flow around a circular cylinder in a hydrodynamic tunnel. Natural temperature gradients existing in the water are sufficient to induce variations in the refractive index exhibited by the wake flow downstream from the cylinder and it is possible to increase the schlieren observations by thermally marking large-scale structures [5].

Box 1 - Schlieren technique

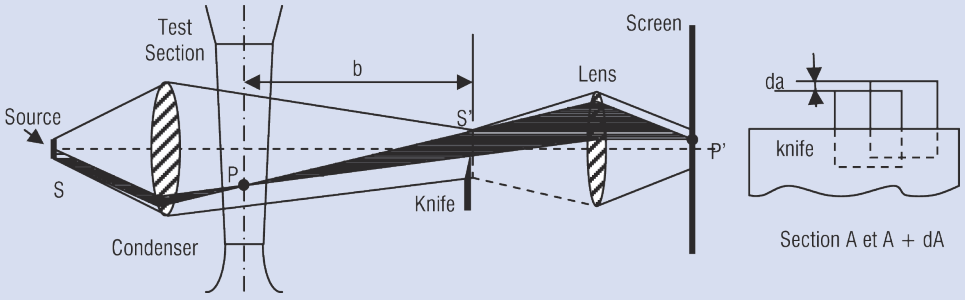

Methods of light deviation : $\theta_x = dE/dx$ or $\theta_y = dE/dy$
Optical thickness : $E = (n-1).e$ e: test section width
Gladstone-Dale relation : $(n-1)/(\rho/\rho_s) = K$ $K = 296.10^{-6}$ (air) and ρ_s : standard gas density
Shadow technique : dI/I // to dn^2/dx^2 or dn^2/dy^2
Schlieren technique: dI/I // to dn/dx or dn/dy

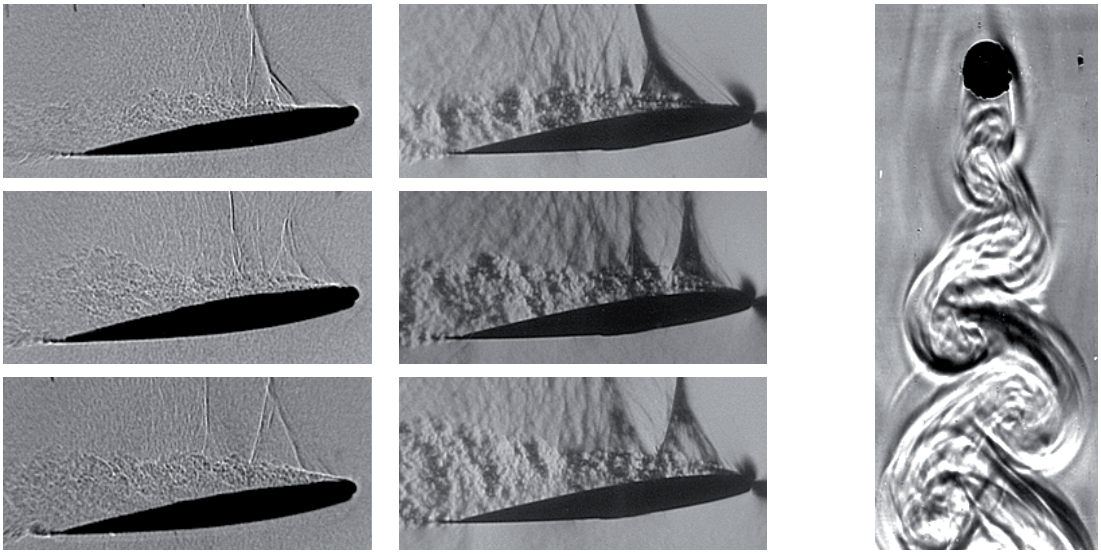

Shadow technique | Schlieren technique | Water tunnel

Figure 2 - Schlieren technique applied to aerodynamic and hydrodynamic flow.

Background Oriented Schlieren technique : a simple quantitative schlieren method

The Background Oriented Schlieren (BOS) technique [6] is one of the most recent schlieren techniques. This method likewise takes advantage of a very simple phenomenon: the mirage effect. The basic principle of the BOS thus consists of imaging a structured scene, preferably a dot-pattern, observed through the flow of interest. The refractive index variations in the flow make the images of the dotted points move. The displacement d of each individual image corresponds to a light deflection angle ε in two spatial directions (Figure 3). The deflection angle is given by:

$$\varepsilon = -\frac{d \times p}{D} \qquad (3)$$

where p is the physical dimension of a pixel in the dot-pattern background and D the distance between the background pattern and the intersection point between the undisturbed and disturbed light rays. This technique is thus sensitive to the density gradient vector field. In contrast to the classical schlieren methods, digital image processing replaces the optical processing to compare the schlieren distorted and undistorted image of the pattern background. The image correlation PIV technique is used to derive the projected mass density gradients in the observing direction.
The main value of the technique is that it can be applied to visualize large fields of interest in wind tunnels but also in outdoor experiments with simplified experimental equipment, eliminating the need for high-quality optics and windows, knife-edges, and laser sources. In its simplest form, this low-cost method requires a structured, randomly-generated background pattern, a high-speed camera and a high-intensity light source to illuminate the scene (Figure 4).

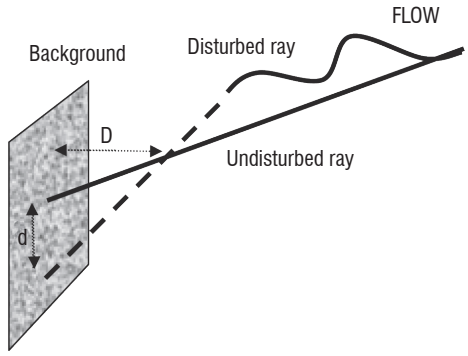

Figure 3 - Schematic of the BOS principle

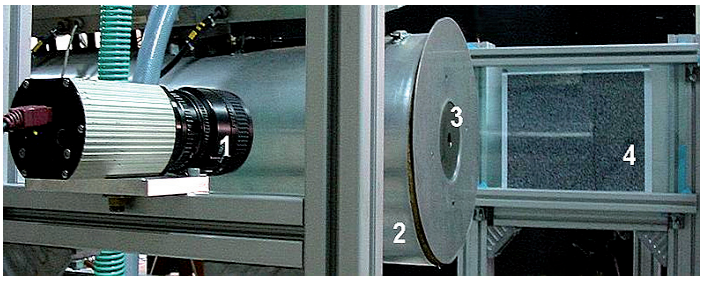

Figure 4 - BOS set-up with camera and dot-pattern background for studying supersonic jets.
1: Camera sensor, 2: Supersonic jet nozzle, 3: Duct , 4: Dot-pattern scene

Further quantitative density measurements can be obtained in the same manner by using another schlieren technique. The BOS technique was implemented at Onera to study the aerothermal effects of hot supersonic jets [7]. Quantification of the jet turbulence was derived from BOS measurements using the Abel transform under the assumption of an axisymmetric jet (Figure 5).

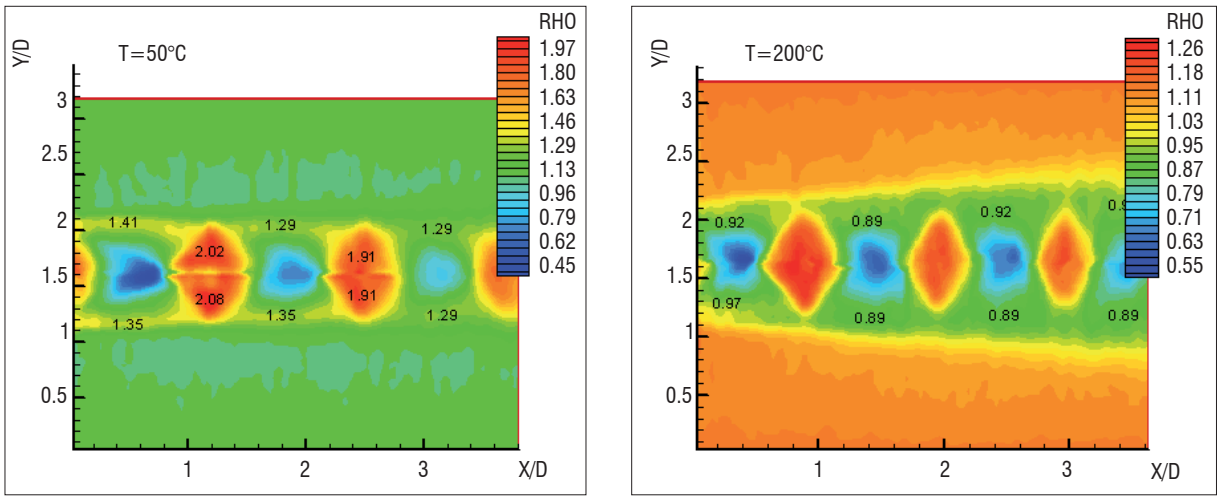

Figure 5 - Mass-density fields of the mixing zone in a hot supersonic jet at T=50°C and at T= 200°C

The size of the turbulent mixing zone dramatically increases downstream at high temperature. The application of the BOS technique was also successfully demonstrated by the DLR through investigations on compressible vortex formations from the blade tips of two different helicopters in flight [8].

Differential interferometry or color schlieren technique

In the observation and analysis of high-speed flows, monochromatic interferometry has been developed to obtain quantitative information about gas density in large fields [9]. When density gradients are relatively weak, differential interferometry in polarized white light is very well suited [10], [11]. Briefly, a Wollaston prism decomposes a light wave polarized in a given direction into two orthogonal vibrations of approximately equal amplitudes separated by a small birefringence angle ε. The prism is placed at the center of curvature of a spherical mirror placed behind the test section. After crossing it, the beam is focused back towards the source, thus crossing it a second time, so that the sensitivity is increased. This is a compensating device, as the initial path difference between the two rays can have an arbitrary value, thus yielding a uniform color on the screen, simply by translation of the prism. It is also self-compensating because, the prism being fixed, any deviation of the light rays produces optical path lengths in the air and prism which compensate for each other. In white light, a colored fringe pattern can be observed in a sequence approximately matching Newton's color scale. The prism used is of the wide-field type (see Box 2), which yields a uniform background tint in a convergent light beam. The apparatus is easy to set up and it has a high sensitivity and is much smaller and less subject to vibrations than the conventional separated-beam interferometers such as the Mach-Zehnder interferometer.

Application to 2D-unsteady wake flows

In this example, the unsteady wake flow is analyzed behind schematic turbine blades at Mach 0.4 [12]. The unsteady pressure signals are simultaneously recorded around the trailing edge in order to be able to synchronize pictures and pressure variations. Two successive interferograms and the gas density field are given in Figure 6. The gas density ρ is referenced to the upstream gas density ρ_∞. With this model, the trailing edge is circular and 15 mm in diameter and the boundary layer state is quasi-laminar. In fact, because of the shifting of the two interfering rays, the interferograms cannot be analyzed down to the model wall. For example, an analysis conducted following a vertical line is only possible until one of two interfering rays is blocked by the model. In the conditions of the optical setup, the analysis is made down to 1.57 mm from the model wall and the gas density at the wall is obtained through extrapolation of the data. The density fields of Figure 6 show the vortices as concentric rings, with density decreasing toward the center. These vortices pass through a formation phase where the density decreases in the vortex center and a dissipation phase where the density and the size of the vortex increase.

Box 2 - Large-field Wollaston prism

n_e : extraordinary refractive index
n_0 : ordinary refractive index
α : pasted prism angle
ε : birefringence angle

$\varepsilon = 2.(n_e - n_0).\tan\alpha$
Measurement sensitivity depends on the birefringence angle

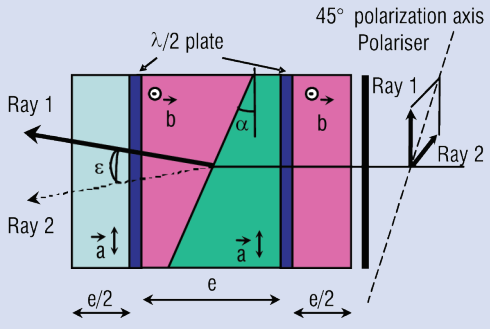

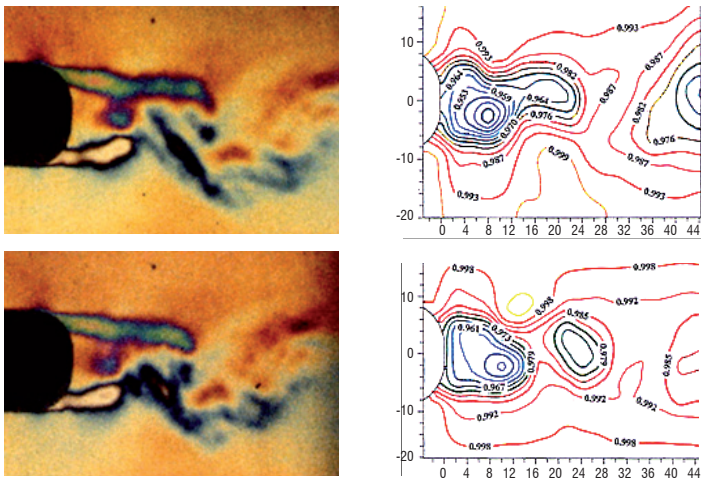

Figure 6 - High speed interferograms and gas density field reconstruction $\Delta t = 50\ \mu s$, M = 0.4

Application to axisymmetric wake flows

Differential interferometry is a non-intrusive technique that is particularly well-suited to investigation of phenomena related to compressibility and high temperatures. In the case of axisymmetric wake flows, it has been used to analyze the structure of a hot supersonic jet at Mach 1.8 injected into a coaxial supersonic flow at Mach 1.5. The method is sufficiently sensitive for a quantitative analysis to reconstruct the local density field. This operation is possible from a single interferogram provided the flow is two-dimensional or axisymmetric. The flow structure was assumed axisymmetric [13] and the interferograms were recorded with horizontal fringes, so that vertical gradients of the refractive index are detected. The radial density distribution was determined by spectrum analysis of the colors in the upper half-plane. Wherever possible, a similar analysis was made for the lower half-plane to see whether the flow was effectively axisymmetric. The axisymmetric flow was reconstructed from the undisturbed flow starting as close as possible to the axis of revolution.

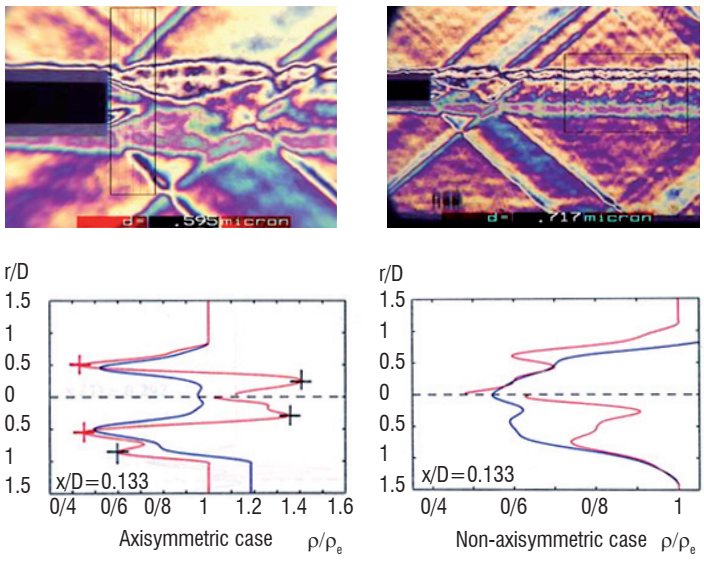

Figure 7 - Interferograms of the jet and radial distribution of the gas density.

Figure 7 shows two interferograms recorded for two different pressure ratios of 2.74 and 3.38 at the same temperature ratio of 1.67. In the analysis of the interferograms, the density distributions were computed along vertical lines. Whenever the vertical line, where the analysis is performed, completely crosses the jet, a density profile can be determined by integration in the upper half-plane and in the lower-plane. If the flow is strictly axisymmetric, the two profiles should be identical. In Figure 7 and for the axisymmetric case, the profiles of the optical thickness (blue line) and the gas density (red line) obtained near the nozzle exit section are relatively symmetric around the flow axis. In the non-axisymmetric case, the analysis made far downstream provides relatively contrasted density profiles which reflect the presence of local turbulences in the flow.

Application to hypersonic wake flows

In a hypersonic wind tunnel, the difficulty in measuring gas density is due to the fact that the index variations to be measured in the test section are very small. There are two reasons for this. Firstly, the light deviations are produced by beams that are passing through a phenomenon that is axisymmetric, and not two-dimensional. The integration paths traveled by the beams are therefore shorter, especially in the close vicinity of the shock. Secondly, since the free stream mass density is low (on the order of 2.10^{-2} kg/m^3), the index variations caused by the mass density gradients in the passage through the shock waves will induce index variations that remain very small (Box 3). The example presented consists of analyzing hypersonic flows around slender axisymmetrical bodies in order to compare the gas density distributions obtained in the shock layers with the analytical solutions [14]. Here, the Wollaston prism used separates the partial beams very widely. The prism angle itself is about 18° so that the distance between the two partial beams is 14.60 mm at the level of the spherical mirror, and it is therefore greater than the domain to be measured. This is equivalent to an ordinary interferometry arrangement with a separate reference, because the interferogram is directly interpretable in a two-dimensional flow but the setup is still differential because one of the beams, used as a reference, is placed in the undisturbed flow, either upstream from the model or, as in the present case, on the side of the model, outside of the shock layers. The interference fringes are placed horizontally so that the separation between the two beams will be vertical. The radial distribution of the mass density shown in Figure 8 has been obtained in the shock layer that develops around a cone of length $L = 300$ mm and apex semi-angle $\theta_c = 11.5°$. Results show that they are in good agreement with the analytical solutions on slender ogives following Merlen and Andriamanalina's power law and Jones' tabulated data for an inviscid flow of ideal gas around a cone.

Box 3 - Optical limit of differential interferometry

Minimum phase difference δ_{min} detected : 30.10^{-9}m
(from Gontier [10])

Optical thickness difference : $\Delta E = \delta_{min} / 2$
(double crossing of test section e)

For e = 40 mm (width of the test section) : $\Delta\rho_{min} = 1.64.10^{-3}$ kg/m^3

For e = 150 mm (width of the test section): $\Delta\rho_{min} = 4.4.10^{-4}$ kg/m^3

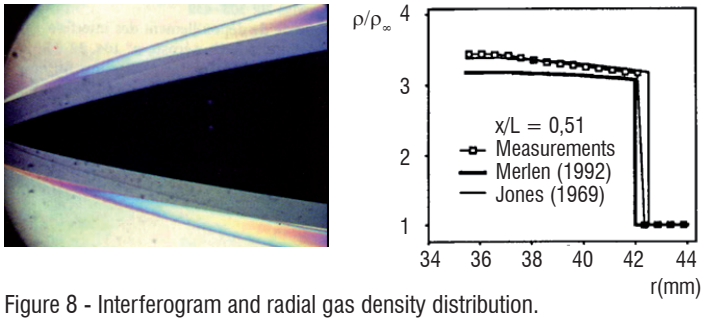

Figure 8 - Interferogram and radial gas density distribution.

Application to gaseous mixture

Differential interferometry has also been used to analyze the stability of the interface separating two fluids of highly different densities when it is impacted by an incoming shock wave [15]. The shock tube is vertical in order to keep the interface stable before the arrival of the shock wave. In this test, two diagnostic techniques are compared: X-ray densitometry and differential interferometry. For the X-ray technique, the partial gas density profile of one of the two gases can be obtained with careful calibration if the gas pair is air/xenon. In the case of SF6/air, both gases are transparent to X-rays and radiography cannot be used. Only differential interferometry can yield a measurement of SF6 distribution in air. The optical setup requires two Wollaston prisms (0.5° pasted angle) installed head to foot and two "Clairaut" achromatic lenses, 800 mm in focal length and 120 mm in diameter.

In the case of two-gas mixtures, Merzkirch has shown that the Gladstone-Dale relation can be extended if the Gladstone-Dale constants of each gas are known [11]. Then, the analysis of the interferogram yields the partial density profile of one of the two gases across the interface. Figure 9 shows three interferograms recorded at different times. On the interferogram (a), the shock wave has already crossed the interface, has been reflected from the tube end wall and is about to again impact on the modified interface. Picture (b) was taken shortly after this second impact and the wave is seen to have been partly transmitted into SF6 and partly reflected into the air. On picture (c) the transmitted wave can be seen close to the bottom of the picture while the reflected part has again been reflected from the end wall and is about to impact on the interface.

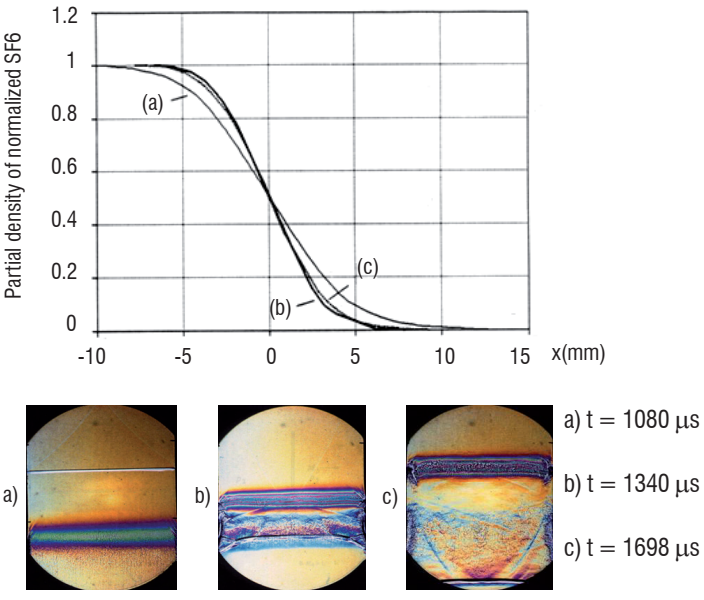

Figure 9 - Gas density profiles of SF6 6 - Interface: SF6-Air, Ms = 1.45.

The SF6 partial density profiles were obtained through the interface by averaging a dozen interferograms. For the xenon/air gas pair, the xenon partial density profiles were compared to those obtained by the X-ray technique. The two techniques yield very similar results (Box 4).

Box 4 - Galdstone-Dale relation in gas mixture

If ρ_1 and ρ_2 are partial gas densities:

$$n-1=K\rho=K_1\rho_1+K_2\rho_2$$

Interferogram analysis yields:

$$n(y)-n_L=(n(y)-1)-(n_L-1)=\frac{\int\theta_y.dy}{L}$$

L : test section width
n_L : refractive index of reference gas
$n_1(y)$ through the interface :

$$n_1(y)-1=\left[1-\frac{(n(y)-1)-(n_L-1)}{(n-1)_{\max}-(n_L-1)}\right](n_L-1)$$

and then the partial gas density profile:

$$\rho_1(y)=\frac{(n_1(y)-1)}{K_1}$$

Real-time true-color holographic interferometry

The use of differential interferometry implies data integration to get the full gas density and this integration results in a certain measurement inaccuracy. To obtain absolute data, Onera developed real-time true color holographic interferometry using a three-color laser source [16]. As shown in Figure10, the interference fringe patterns versus the optical path difference are compared for three different sources. With a xenon light source (a), the central white fringe visualizes the zero order deformation and small path differences are correctly measured but above several micrometers, the tints are no longer distinguishable and large path differences cannot be measured. With a monochromatic laser source (b), the central white fringe (zero order) can never be identified and it is not possible to follow the displacement of the fringes through a shock wave. But, when it is possible to count the fringe number, large path differences can be measured. With a three-laser source (c), the zero order is always identifiable (white fringe) and the colors always remain identifiable for small and large path differences.

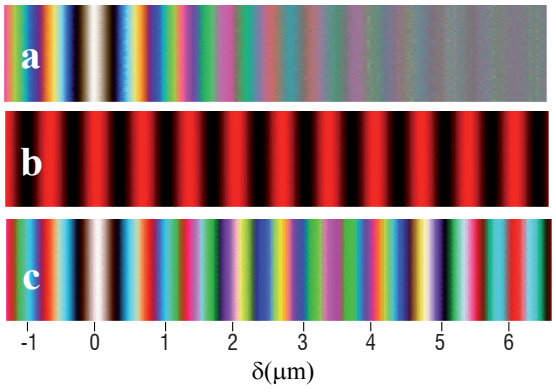

Figure 10 - Color of interference fringes.

Transmission hologram

The feasibility of this technique was confirmed with the Research Institute of Saint-Louis (ISL) and applied in several Onera wind tunnels. Figure 11 shows the optical setup using single-layer panchromatic holograms recorded by transmission. A reference hologram made without flow records the interferences between the three reference waves and the three measurement waves. It is then developed and is replaced on the setup. If a change in optical path is created in the test section, color variations representing the phenomenon will be visualized in real time behind the hologram. The flow studied was the unsteady flow downstream from a cylinder of 20 mm in diameter placed crosswise in the test section at Mach 0.37. High speed interferograms were recorded with a rotating-drum camera at high frame rate (30,000 f/s) and the exposure time of each interferogram was 750 nanoseconds. On the interferogram of Figure 11 we see that each vortex is defined by concentric rings where each color visualizes an isochore line. These colors were analyzed using proprietary software [17] to find the vortex position and velocity and the evolution over time of the gas density field.

Reflection hologram

To increase the diffraction efficiency of a hologram, which is about a few percent in transmission, Onera created an optical bench that uses reflection holograms. In transmission however, the interference fringes are set down perpendicular to the plate and a small variation in gelatin thickness caused by the chemical treatment of the hologram does not modify the three interfringes. In reflection on the other hand, the interference fringes are recorded parallel to the plate surface and the interfringes are very sensitive to small variations of gelatin thickness. Solutions were proposed to control the gelatin shrinkage. Very good results were obtained with narrowed fringes and a uniform background at Mach 0.45 around the same circular cylinder [18]. In the setup in Figure 12, the holographic plate is set in the front of the test section and, at the first exposure without flow, it records the interferences between the incoming rays and the rays reflected by the flat mirror located just behind the test section. As the hologram simultaneously records the interferences of the three wavelengths, the diffraction efficiency of the three gratings becomes close to 50%. This value is very important because, at the second exposure, as the diffraction efficiency is close to 50%, 50% of the light is reflected by the hologram and constitutes the three reference waves. The other 50 % crosses the test section twice and interferes in real-time with the three reference waves. Interference fringes are not localized because they can be observed from the holographic plate to the camera. If no disturbances exist in the test section, a uniform background color is obtained in the camera. If variation in the refractive index exists in the test section, it will be seen on the screen. This original arrangement constitutes the first real-time, three-color holographic interferometer using reflection holograms and the holograms obtained exhibit well-saturated and more contrasted colors than those obtained in previous experiments performed with transmission holograms. That makes the quasi-automatic analysis of interferograms easier.

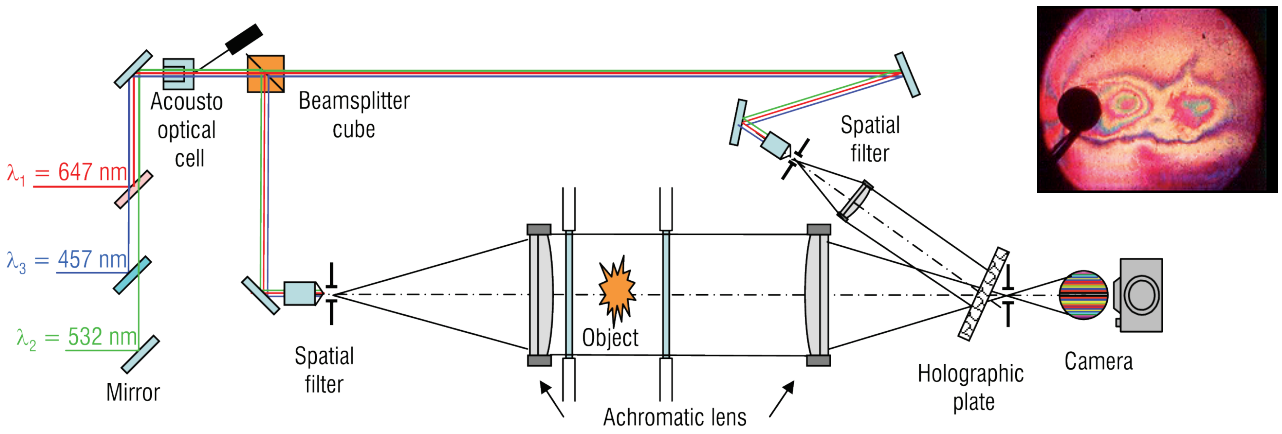

Figure 11 - Real-time three-wavelength transmission holographic interferometry
Video - http://aerospacelab.onera.org

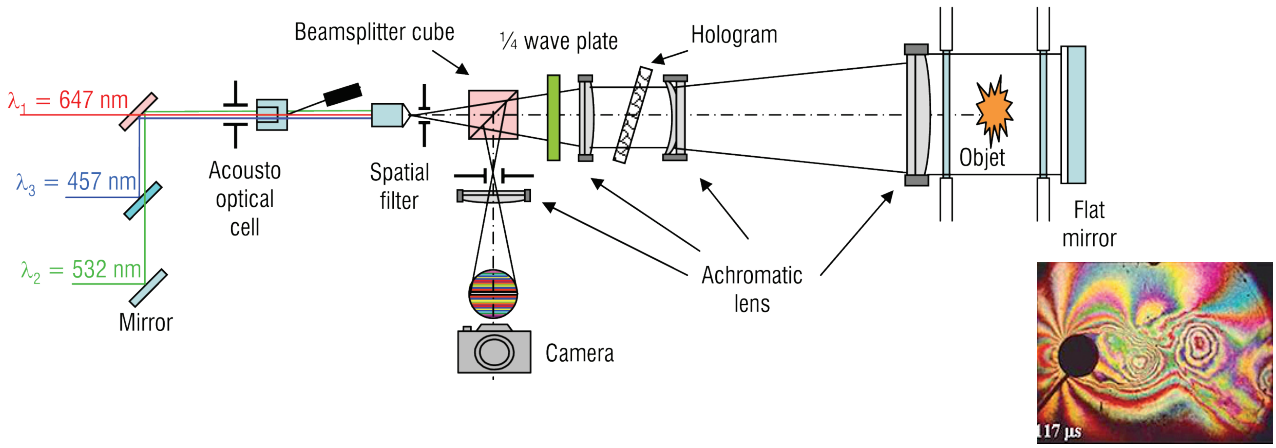

Figure 12 - Real-time three-wavelength reflection holographic interferometry
Video - http://aerospacelab.onera.org

Digital color holographic interferometry

One possibility for avoiding holographic plates and chemical processing is related to digital three-color holographic interferometry. Technological improvements in the field of matrix sensors offer new possibilities for holography. Hologram recordings can be done using CCD matrices with increased resolution and greater digital gain. For this reason, the feasibility of the digital three-color holographic interferometer was designed to analyze the variations in refractive index induced by a candle flame [19]. Color holograms are generated and recorded with a three-layer photodiode stack sensor allowing for simultaneous recording with high spatial resolution. Phase maps are calculated using a Fourier transform and spectral filtering are applied to eliminate parasitic diffraction orders (see Box 5). From the phase differences, it is possible to calculate the intensities of interferences induced by the flame in the RGB colors calculated. The optical bench used and the results in the case of the candle flame are presented in Figure 13. Zero order fringe (white fringe), meaning zero optical path difference, can be easily extracted from the experimental data by considering the wrapped phases along the three wavelengths. The use of three colors is of great value if one looks at precisely the background tint observed outside the flame. In normal experimental conditions, the synthesized background color should be represented in white ($\delta = 0$) if there has been no disturbance between the reference and the probe recordings. In Figure 13, it can be seen that the white fringe is shifted and located inside the flame (see zoom of flame). This means that the background pattern has moved slightly between the reference and probe recording. This feature was not observed in experiments based on single wavelength interference and shows the value of using color in digital holographic interferometry.

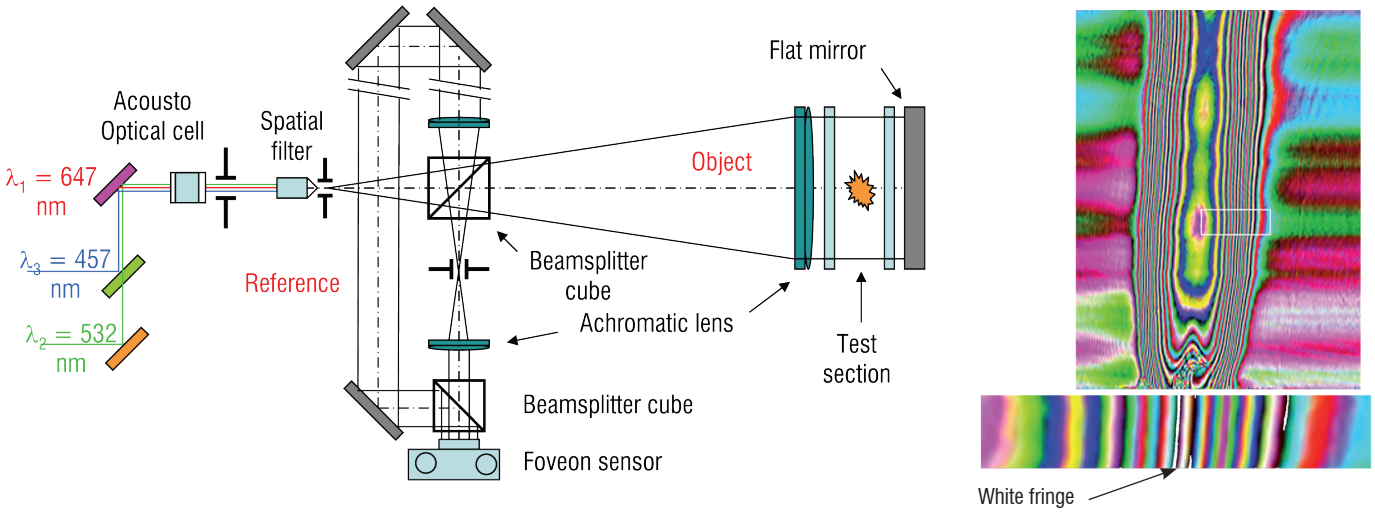

Figure 13 - Digital three-color holographic interferometer and application to flame.

Box 5 - Off-axis hologram analysis by direct and inverse 2D FFT algorithms

- Image plane hologram can be expressed: $H_\lambda(x,y) = O_0(x,y) + b_\lambda(x,y)\exp\left[i\phi_\lambda(x,y)\right]\exp\left[2i\pi\left(u_\lambda x + v_\lambda y\right)\right] + b_\lambda(x,y)\exp\left[-i\phi_\lambda(x,y)\right]\exp\left[-2i\pi\left(u_\lambda x + v_\lambda y\right)\right]$

where $2\pi(u_\lambda x + v_\lambda y)$ is the spatial carrier modulation along xy.

- Fourier transform gives: $\tilde{H}_\lambda(u,v) = A_\lambda(u,v) + C_\lambda(u-u_\lambda, v-v_\lambda) + C_\lambda^*(u+u_\lambda, v+v_\lambda)$

where $C_\lambda(u,v)$ and $A_\lambda(u,v)$ are the Fourier transform of $b_\lambda(x,y)\exp\left[\mathrm{i}\phi_\lambda(x,y)\right]$ and $O_o(x,y)$.

- Inverse Fourier transform gives: $\hat{c}_\lambda(x,y) \cong \left\{b_\lambda(x,y)\exp\left[i\phi_\lambda(x,y)\right]\exp\left[2i\pi\left(u_\lambda x + v_\lambda y\right)\right]\right\} * h(x,y)$

where * means convolution and h(x,y) the impulse response.

- At any wavelength λ, the phase is given by: $\xi_\lambda^P(x,y) = \phi_\lambda(x,y) + \Delta\phi_\lambda(x,y) + 2\pi u_\lambda x + 2\pi v_\lambda y$

- The phase change between the two states of the object is simply obtained by computing

$\Delta\phi_\lambda(x,y) = \xi_\lambda^P(x,y) - \xi_\lambda^R(x,y)$ and the optical path difference is given by: $\delta = \frac{\lambda}{4\pi}\Delta\phi_\lambda$

A comparison can be made between digital and image color holographic interferometry for the previously obtained results [18-19]. In image color holographic interferometry, a panchromatic holographic plate (7,000 to 10,000 l/mm in spatial resolution) must be illuminated with a total energy of 600 μJ and the coherence length of the three lasers must be more than 2 m. Each interferogram has to be digitized and processed. It is important to obtain a reference hologram of about 50% diffraction efficiency for the three lines and the implementation of the optical setup is not very easy. In digital color holographic interferometry, an energy of 1μJ is sufficient to illuminate the Foveon sensor (200 l/mm in resolution). The laser length coherence can be reduced to several centimeters and some problems can be encountered with the RGB filters overlapping. The implementation is easy enough and the phase difference is entirely estimated with a computer.

Conclusion

Computational fluid dynamics need to be validated by fine measurements in a smaller space or shorter time, or both at once. That is why Onera has devoted much time to developing optical methods based on differential or color interferometry. For shadow and schlieren measurements, these techniques are very easy to implement and they will always yield qualitative data and help with the understanding of unsteady and complex flows. But, if quantitative data are required, color interferometry or color holographic interferometry will continue to be used due to the high resolution of holographic plates. In near future, digital three-wavelength holographic interferometry seems the best candidate to characterize the future complex flows. Although CCD resolution and size are not as good as that of holographic plates, the digital approach is more accessible and versatile since the time for the hologram processing is greatly reduced and the processing is purely numerical.

On the other hand, the value of using color has been demonstrated as the zero order fringe can be easily determined and the variation in the background color due to disturbances can be quantified. The limitations of the method lie in the wide spectral sensitivity of the sensor which produces light diffusion in each monochromatic hologram. Work is currently in progress for removing the color diffusion using a segmentation approach. Success in this strategy will allow for wide spatial filtering, increasing the spatial resolution in the reconstructed object.

Future work will focus on the extension of the proposed technique for analyzing 3D unsteady wake flows. At present, a specific setup of digital holographic interferometry has been defined in a single sight direction, and the aim will be to reproduce the same optical setup along several sight directions, each shifted by a given angle. It is obvious that the optical setup can be reproduced no more than three or four times. But the lake of sight directions should be compensated by high tomographic interferogram resolution for the reconstruction of the 3D gas density field ■

References

[1] G. S. SETTLES - *Schlieren and Shadowgraph Techniques, Visualizing Phenomena in Transparent Media.* Ed. Springer, 2001.

[2] O. RODRIGUEZ - *The Circular Cylinder in Subsonic and Transonic Flow.* AIAA Journal, vol. 22, n° 12, pp. 1713-1718, 1984.

[3] J.M. DESSE - *Influence of Flight Parameters on Air Intake Internal Flow Distortions due to Gun Blast-Air Interaction.* La Recherche Aérospatiale, n° 4, pp. 1-10, 1991.

[4] H. SCHARDIN - *Schlieren Methods and their Applications.* Report TT-F-12731, NASA, Washington, DC, 1970.

[5] O. RODRIGUEZ - *Base Drag Reduction by Control of the Three-Dimensional Unsteady Vortical Structures.* Experiments in Fluids, n° 11, pp. 218-226, 1991.

[6] G.E.A. MEIER - *Hintergrund Schlierenmessverfahren, Deutsche Patentmeldung.* DE 199 42 856 A1, 1999.

[7] C. BARTHE, F. MICHELI, P. MILLAN - *Etude aérothermique de jets supersoniques chauds.* Congrès francophone de techniques laser, CFTL, Toulouse, 2006.

[8] M. RAFFEL, C. TUNG, H. RICHARD, Y. Yu and G.E.A. MEIER - *Background Oriented Stereoscopic Schlieren Helicopter Vortex Characterization*. Proc. 9th Int. Symposium on Flow visualization, Edinburgh, 2000.

[9] C.M. WEST - *Holographic Interferometry.* Ed. Wiley-Interscience, New-York, 1978.

[10] G. GONTIER - *Contribution à l'étude de l'interférométrie différentielle à biprisme de Wollaston.* Publication Scientifique et Technique du Ministère de l'Air, n° 338, 1957.

[11] W. MERZKIRCH - *Flow Visualization*. New-York, Academic Press, 1974.

[12] C.H. SIEVERDING, G. CICATELLI, J.M. DESSE, M. MEINKE and P. ZUNINO - *Experimental and Numerical Investigation of Time-Varying Wakes Behind Turbine Blades.* Notes on Numerical Fluid Mechanics, Vol. 67, Community Research in Aeronautics, 1999.

[13] O. RODRIGUEZ, J.M. DESSE, J. PRUVOST - *Interaction between a Supersonic Hot Jet and a Coaxial Supersonic Flow.* Aerospace Science and Technology, n° 6, pp. 369-379, 1997.

[14] J.M. DESSE, E. FABRE - *Differential Interferometry for Studying Hypersonic Flows.* Experiments in Fluids, n° 20, pp. 273-278, 1996.

[15] I. GALAMETZ - *Visualisation et mesure de masse volumique dans un mélange gazeux en tube à choc.* Thèse de doctorat, Université de Lille, 1994.

[16] J.M. DESSE, F. ALBE, J.L. TRIBILLON - *Real Time Color Holographic Interferometry.* Applied Optics: Vol. 41, n° 25, pp. 5326-5333, 2002.

[17] J.M. DESSE - *Recording and Processing of Interferograms by Spectral Characterization of the Interferometric Setup.* Experiments in Fluids, vol. 23, pp. 265-271, 1997.

[18] J.M. DESSE, J.L. TRIBILLON - *Real-Time Colour Denisyuk Setup for Analyzing High Speed Flows.* Speckle Metrology 2006, Nimes, September 13-15, 2006.

[19] J.M. DESSE, P. PICART, P. TANKAM - *Digital Three-Color Holographic Interferometry for Flow Analysis.* Optics Express, Vol. 16, n° 8, pp. 5471-5480, 2008.

Acronyms

BOS (Background Oriented Schlieren)

Jean-Michel Desse, doctor/engineer, is working at Onera from 1979 in the Applied Aerodynamic Department. His research interests the development of high speed non invasive optical methods based on the refractive index variations in wake flows. Specialist of color interferometry in polarized white light and polychromatic light, his work are now oriented on digital holographic interferometry using three different wavelengths for studying unsteady wake flows.

Ruy Deron received the PhD degree in Automatic and Signal Processing from the University of Nice in 1983. He joined the French National Establishment for Aerospace Research (Onera) in 1984. Since 1990, he has managed experiments dealing with propagation through atmospheric turbulence: laser guide star and ground-based satellite observation, airborne IR imagery. In 2001, he became project manager for an Onera 4 year funded project on aero-optical effects (wind-tunnel experiments and LES simulations). In 2004, he became involved in multi-code development and validation in an aero-thermo-optical 3 year DGA funded project, which he took over for the last year. He is also working in a European working group on optical plume effects.